Comparing Performance of General Rolled Steel and 3D Printed 316L Stainless Steel

Yao-Tsung Lin , Ming-Yi Tsai , Shih-Yu Yen , Guan-Hua Lung , Jin-Ting Yei , Kuo-Jen Hsu , Kai-Jung Chen *

Posted Date: 12 February 2024

doi: 10.20944/preprints202402.0610.v1

Keywords: additive manufacturing; subtractive manufacturing; metal 3D printing; surface roughness; general rolled steel

Article

Comparing Performance of General Rolled Steel and 3D Printed 316L Stainless Steel

Yao-Tsung Lin [1], Ming-Yi Tsai [2], Shih-Yu Yen [1], Guan-Hua Lung [3], Jin-Ting Yei [3], Kuo-Jen Hsu [2] and Kai-Jung Chen [2,*]

[1] Graduate Institute of Precision Manufacturing, National Chin-Yi University of Technology, No.57, Sec. 2, Zhongshan Rd., Taiping Dist., Taichung 41170, Taiwan (R.O.C.), train@ncut.edu.tw; frankyen2003@gmail.com

[2] Department of Mechanical Engineering, National Chin-Yi University of Technology,No.57, Sec. 2, Zhongshan Rd., Taiping Dist., Taichung 41170, Taiwan (R.O.C.), mytsai@ncut.edu.tw; ray104250603@gmail.com

[3] Department of Mechanical Engineering, Chien Hsin University of Science and Technology, Zhongli Dist., Taoyuan County 320312, Taiwan(R.O.C.), l1060188@rechi.com; land1599512356@yahoo.com.tw

* Correspondence: hskchen5@ncut.edu.tw

Abstract: 3D printing is a non-traditional additive manufacturing process. It is different from the traditional subtractive manufacturing process. It offers exceptional rapid prototyping capabilities and results that traditional subtractive manufacturing methods cannot attain, especially in applications involving curved or intricately shaped components. Despite its advantages, metal 3D printing will face porosity, warpage, and surface roughness issues. These issues will affect the future practical application of the parts indirectly, for example, the structural strength and the parts assembly capability. Therefore, this study compares the qualities of the warpage, weight, and surface rough-ness after milling and grinding processes under the same materials (316L stainless steel) between general rolled steel and 3D additive steel. Experimental results show that 3D printing parts are approximately 13% to 14% lighter than the general rolled steel. The surface roughness performance of 3D printing steel is better than general rolled steel under the same material after milling or grinding processing. The hardness of the 3D printing steel is better than that of the general rolled steel. The research verifies that 3D additive manufacturing can use surface processing to optimize surface performance and achieve the functions of lightness and hardness.

Keywords: additive manufacturing; subtractive manufacturing; metal 3D printing; surface roughness; general rolled steel

1. Introduction

Conventional computer numerically controlled (CNC) processes selectively remove material from a position to create desired geometric shapes, namely subtract manufacture. As subtract manufacture challenging to make the complex curves, micromachine parts. Therefore, a metal laser laminated manufacturing technology was created. That is additive manufacturing [1]. Additive manufacturing (AM) processes is an innovative component manufacturing concept to make the complex curves micro-machines parts. AM processes can mainly be divided into two types. One is powder bed fusion (PBF), and the other is directed energy deposition (DED) [2,3]. Selective laser melting (SLM) is one of the Powder Bed Fusion (PBF) technologies [4], as PBF technology can produce personal, internal flow channels or various products without forming mold or machining tools. Therefore, it has been widely used and studied in recent years.

The metal parts have the advantages of high-temperature, high-pressure, impact, and oil corrosion resistance compared to the traditional glass or plastic parts. Therefore, non-metal materials cannot replace them in some application situations. The surface morphology of PBF

 doi:10.20944/preprints202402.0610.v1

products is usually similar to porous materials, so they are less good than subtract manufacturers in performance, such as the surface finish, porosity, thermal deformation, and residual stress [5–8]. This phenomenon will affect the structure's strength and the surface aesthetic issues. Furthermore, the workpiece's surface performance will affect the tor resistance, lubricating, air tightness, fatigue, and outward appearance [9]. So, controlling surface roughness is necessary for applying metal laser laminated manufac-turing technology.

316L stainless steel is austenitic stainless steel. We also called 316L SS. Due to its ex-cellent mechanical properties and corrosion resistance, it is one of the most frequently used stainless steels. Many 316L SS components have complex geometries, for example, pipeline systems used in the nuclear industry, various tailor-made implants, automotive, kitchen tools, and aerospace industries. They make conventional manufacturing processes difficult and costly. Zhang S. et al. [10] used 316L SS to replace A36 steel to repair the steel bridge beam by 3D printing. The experimental results show 316L SS can improve the ten-sile strength more than the materials of A36 steel. However, the materials of 316L SS have the disadvantage of lower yield strength. Zhang Y. et al. [11] used electron backscatter diffraction and transmission electron microscopy to analyze the deformation behavior when the powder materials of 316L stainless steel (316L SS) are printed microstructure. The results showed that the printing parameters will affect the material behavior of 316L SS under PBF manufacturing. Wang Y.M. et al. [12] optimal the printing parameters to change the density of the part. Moreover, Nath S.D. et al. [13] used laser-powder bed fusion (L-PBF) to compare the mechanical properties when the materials of 420 stainless steel ad-ditives were manufactured and heat treatment operation. The results show that heat treatment can improve the tensile strength, yield strength, and elongation of 420 stainless steel parts in addition to the hardness that cannot be changed. Based on the above de-scription, using post-processing methods to improve performance in metal 3D printing specimens is a worthy issue to study.

This study compares surface roughness quality after grinding processes in the same material (316L stainless steel) between general rolled steel and 3D printed steel. The mo-tivation for comparing surface roughness is its roughness related to the performance of the process in spraying, electroplating, and polishing [14,15]. Once the surface roughness be-comes smooth, the performance and durability after treating the surface of the parts in-crease. This study chose milling and grinding because these methods are usually used in final surface processing. Thus, it is based on the materials of 316 L SS to experiment with improving the surface finish in the 3D additive manufacturing parts. In addition, we also to explore the difference in the hardness, stress and strain between general rolled steel and 3D printed steel. The purpose is to understand the properties in the 3D printed materials and application.

2. Research Methods

The mechanical properties of SLM-fabricated alloys depend on the micro-structure devel-oped during processing [9]. To explore the mechanical behavior of SLM 316 SS, the re-search used the substrate of the 316L SS to explore the difference in the performance of processing and properties by 3D additive manufacturing and subtraction manufacturing.

2.1. Laser 3D Printing Process

Laser 3D printing involves several parameters. Laser power, travel speed, and hatch spacing are three of the most easily manipulated. The hatch pattern, which affects the thermal stress profile, is easy to manage, but the effect is difficult to quantify. Layer-by-layer fabrication causes anisotropy, so building angle or component orientation be-comes essential. Heat input is a function of several parameters. One definition of heat in-put is the energy density (E) as Eq (1) [16].

$$E = \frac{P}{vht} \tag{1}$$

where, P is the laser power in watts, v is the travel speed in mm/s, h is the hatch spacing in mm, and t is the layer thickness in mm.

 doi:10.20944/preprints202402.0610.v1

2.2. Density & Porosity

3D printing is a well-known phenomenon that produces porosities in parts. It will reduce the density of the elements. To improve the density of 3D printing parts, it is crucial to assess the physical origin of the different types of porosities and to measure the porosity rate as precisely as possible so that one may select the optimum manufacturing parameters. Porosity can be measured by Archimedes' measurement [5]. The density of the fluid is ρ_{fluid}, and the air is ρ_{air} if we know the mass of the specimen in the air (M_{air}) and the liquid (M_{fluid}). It becomes possible to calculate the density of the specimen. The formulas are Eq. (2) and Eq. (3).

$$\rho_{specimen} = \frac{M_{air}}{(M_{air} - M_{fluid})} \times (\rho_{fluid} - \rho_{air}) + \rho_{air} \quad (2)$$

$$Porosity = 1 - (\frac{\rho_{measured}}{\rho_{theoretical}}) \quad (3)$$

where $\rho_{measured}$ represent the measured density and $\rho_{theoretical}$ represent the theoretical density.

2.3. Experimental Materials

The study used the powder of Tongtai Corp. SS-316L to do the metal 3D printing ma-terials. The manufacturer number is 3354574. The metal particle size is shown in Figure 1 illustration. The most particle size distribution is about 36.5±15.5μm. Figure 2a is the schematic diagram of the metal 3D printing. The metal 3D printing facilities used Tongtai AMP-160 to print tensile and block specimens. Table 1 shows the printing processing parameters [17].

Table 1. Processing parameters of specimen by SLM manufactured.

	Laser Power **Watt**	**Scanning Speed** **mm/s**	**Laser diameter** **μm**
Border	100	250	0.1
Hatches	100	250	0.1
In skin			
Blocked path	220	900	0.1
Border	220	900	50
Additional border	220	900	50
Fill contour	220	900	50
Hatches	220	900	50
Down skin			
Blocked path	100	900	50
Border	220	900	50
Additional border	100	900	50
Hatches	220	900	50
First layer			
Blocked path	100	250	1
Border	100	250	1
Additional border	100	250	1
Fill contour	100	250	1

 doi:10.20944/preprints202402.0610.v1

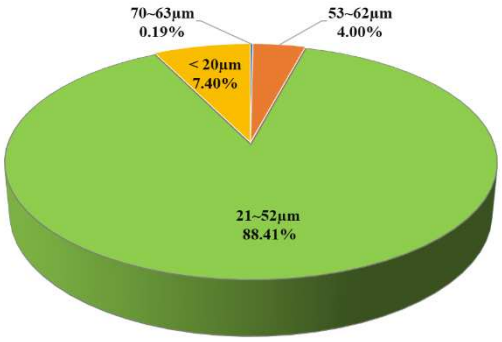

Figure 1. The particle size distribution percentage with the powder of metal 3D printing.

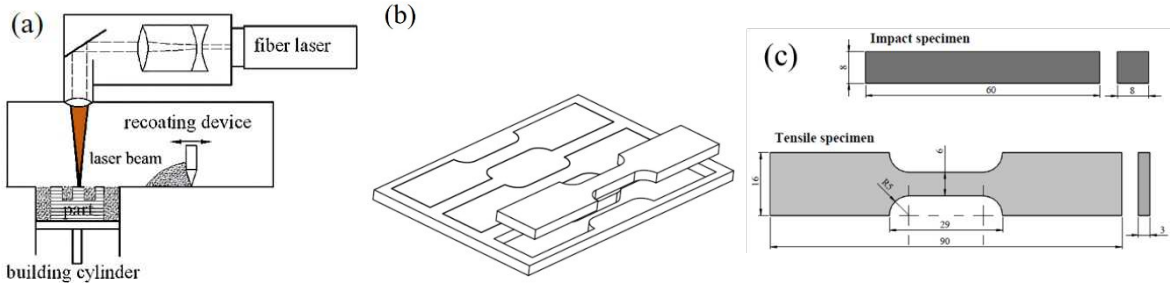

Figure 2. Additive and subtractive manufacturing with 316L stainless steel. (a).Additive manufacturing was used to PBF process, (b).Subtractive manufacturing was used to CO_2 laser cut, (c).Specimen scale.

3D additive and subtractive manufacturing will produce warpage and distortion due to the hot and cold variation in processing [18]. Figure 2b is the schematic diagram of subtractive manufacturing in the SS-316L plate. 3D additive manufacturing is to complete parts by stacking them layer by layer. The materials will drop when printing in the hang-ing place. Therefore, support must be designed in the hanging area [19].

We use tensile specimens to explore the difference in the warpage and distortion when 3D metal printing is in support and non-support designs. The thickness of the ten-sile specimen is 3.0mm. Figure 2c represents the scale of impact and tensile specimens. The scale of impact and tensile specimens are according to the ISO 6892-1 specification to design [20]. Figure 3a,b showed the 3D metal printing specimens with support and non-support designs.

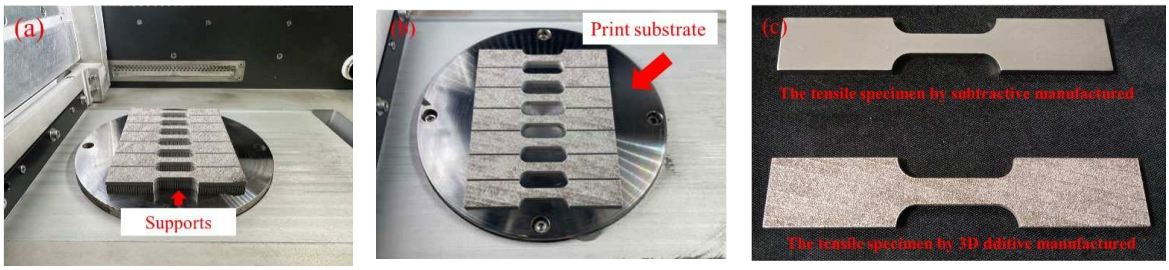

Figure 3. 3D printed in the metal material of 316L stainless (a). 3D printed tensile specimen with the supports. (b). 3D printed without supports design in the tensile specimen. (c). Tensile specimen.

The research also discusses the secondary processing performance with general rolled and 3D printed steel in the 316L SS materials. The experimental specimens are used to the impact specimens to explore the difference in the weight, roughness, and hardness, as shown in Figure 4a,b. The Mitsubishi ML3015 eX-F Plus CO_2 Laser facilities manufactured subtractive manufacture of the impact and tensile specimens. General rolled steel is manufactured by Ycinox Corp. Table 2 shows the chemical compositions of the general rolled steel and 3D printing powder steel of 316L stainless.

 doi:10.20944/preprints202402.0610.v1

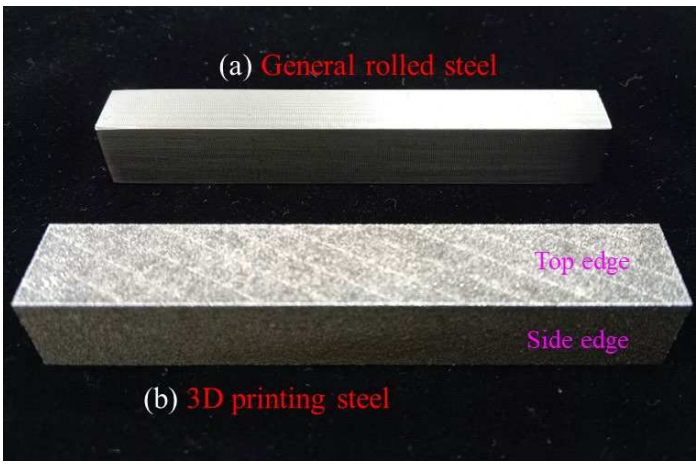

Figure 4. The impact specimens with the material of 316L stainless steel.

Table 2. Chemical compositions of 316L stainless steel.

Material	Fe	Mo	Ni	Mn	Cr	Si	O_2	C	P	S	N
Rolled steel	Bal.	2.1	10.12	1.6	16.74	0.58	-	0.014	0.037	0.002	0.021
3D printing steel	Bal.	2.5	12.7	1.4	16.8	0.7	0.06	0.01	-	-	-

2.4. Surface Roughness

Surface roughness is due to the high-frequency vibration factor producing the irregu-lar surface in the processing [21]. After manufacturing the workpiece, we must measure the surface roughness to confirm the qualities. The research is according to the standard of ISO 25178 to measure the surface roughness of the workpiece [20]. Surface roughness is divided into arithmetic mean deviation Ra and ten-point average roughness Rz [22].

The middle arithmetic deflection of elaborated profile on the basic length Ra. Arithmetic mean deviation can be obtained by taking a standard-length l from the average line direction of the roughness graph. The X-axis is the middle line direction, while the y-axis is the roughness value. Ra is defined as Formula 4 when the roughness graph is y=f(x).

$$\mathrm{Ra} = \frac{1}{l}\int_0^l f(x)dx \tag{4}$$

Ten-point average roughness Rz. Ten-point average roughness is obtained by taking a standard-length *l* from the average line direction of the roughness graph. The longitudinal direction is the expression of the roughness value. The sum of the averages can be obtained by adding the absolute mean value of the highest peak to the 5th peak y_p and the absolute mean value of the most bottom to the 5th bottom y_v. Rz is defined as:

$$\mathrm{Rz} = \frac{\left|y_{p_1} + y_{p2} + y_{p3} + y_{p4} + y_{p5}\right| + \left|y_{v1} + y_{v2} + y_{v3} + y_{v4} + y_{v5}\right|}{5} \tag{5}$$

In addition, the measurement of the surface roughness in the metal has been widely presented with 3D geometric shapes in recent years [9]. Therefore, the workpiece's surface morphology can be given as Sa, Sq, and Sz. Sa represents the absolute mean value relative to the height difference at each point of the measurement surface. The formula is given as (6).

$$S_a = \frac{1}{A}\int\int |Z(x,y)|dxdy \tag{6}$$

 doi:10.20944/preprints202402.0610.v1

Sq represents the average value of the root mean square in each point height within the measurement range. The formula is given as (7).

$$S_q = \sqrt{\frac{1}{A}\iint_A Z^2(x,y)dxdy} \quad (7)$$

Sz represents the sum of the maximum height peak and the total depth trough within the measurement range. The formula is given as (8).

$$S_z = \max_A Z(x,y) + \min_A Z(x,y) \quad (8)$$

3. Results and Discussion

3.1. Warpage and Distortion Analysis

Support scaffolding is used to aid support when the materials are under the floating state in additive printing. For example, the process is printing shell or surface [23,34]. In addition, the workpiece will produce warpage and distortion after the selective laser melt-ing processing [2]. Therefore, we used the simulation and experimental software to inves-tigate the phenomenon of warpage and distortion when the specimen additive was manu-factured with support and non-support scaffolding. The measurement facilities use KEYENCE VR-6000 3D optical profilometer to measure the warping and distortion in the tensile specimen after the tensile specimen of the 316L SS manufactured by 3D additive and subtract processing. Figure 5 shows the simulation results of the tensile specimen 3D additive manufacturing process. Figure 5a was designed with support scaffolding, and the height of the support scaffolding was designed to be 3.0mm. Figure 5b was designed without support scaffolding. The software for the simulation is the Ansys workbench. The boundary conditions of the simulation are set according to Table 1. We found the support scaffolding design of the specimen is higher than without support scaffolding design in the index of the warpage and distortion, as shown in Figure 5a,b.

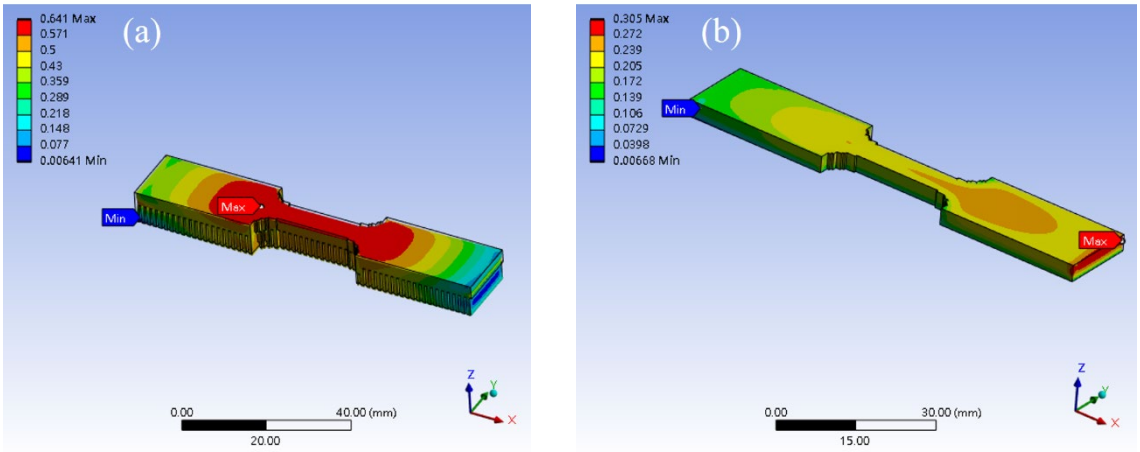

Figure 5. The simulation of 3D additive manufacture specimen with support and non-support scaffolding design. (a) is the support scaffolding design. (b) is the non-support scaffolding design.

Figure 6a,b show the tensile specimen with import support scaffolding and non-support scaffolding design after the 316L SS printed tensile specimen materials. Figure 6c shows the manufactured tensile specimens by laser subtraction. The average value of the warping and distortion is 0.46±0.05mm with support design, and the average value of the warping and distortion is 0.1±0.03mm without support design after the tensile specimen manufactured by 3D additive printed as Figure 6a,b. The average value of the warping and distortion was 0.23±0.03mm when the tensile spec-imens were manufactured by laser subtract processing, as in Figure 6c. We realize that the support scaffolding will cause warping and distortion in the specimens when 3D ad-ditive

 doi:10.20944/preprints202402.0610.v1

processing is done. This is due to the uniform temperature distribution, leading to the warping and distortion in the specimens. It is also called the stress residual in the specimens [25–27].

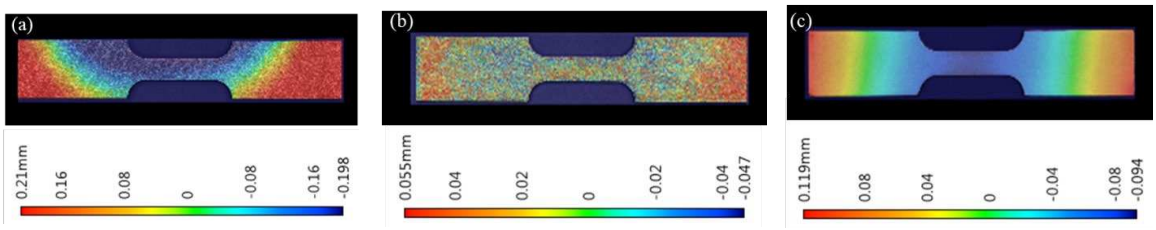

Figure 6. The warpage and distortion in the specimen of 316L staimless steel. (a).Tensile specimen by 3D additive manufactured with supports. (b).Tensile specimen by 3D additive manufactured without supports. (c).Tensile specimen by subtractive manufactured.

3.2. The Porosity Analysis

The metal 3D printed process will face the issue of porosity due to the powder thickness not being uniform [28]. It has been found that the porosities can be optimized by adjusting laser scanning paths and solid solution treatments to control the porosity size. Besides, the porosity will affect the workpiece's weight and the reliability of structural strength [29,30]. The research manufactured tensile and block specimens to explore the weight difference between general rolled steel and 3D printed steel of the same 316L SS materials. The printed parameters were according to Table 2.

Figure 6 shows the experimental results. Figure 7a shows that the weights and measures instrument was under without loading state. Figure 7b shows that the weights and measures instrument was in the loading state. Digital precision weights and measures instrument is manufactured by Nanxing Corp. Figure 7c shows the average weight of the tensile specimens. The blue bar is generally rolled steel, weighing 27.65±0.1g. The or-ange bar is 3D additive steel and weighs 24.04±0.3g. We found the weight of the 3D addi-tive manufactured is lighter by 13.1% than the rolled manufactured when the workpieces were manufactured to tensile specimens. Figure 6d shows the average weight of the block specimens. The weight of general rolled steel is 33.36±0.2g, as shown in the blue bar. The weight of the 3D additive manufactured is 28.75±0.3g, as shown in the orange bar. The 3D additive manufactured steel specimens are lighter, 13.83%, compared to the gen-eral rolled steel. These represent the qualities of the 3D additive manufactured that are near the same in the porosity when the printing process is under the same laser power and scanner speed [28].

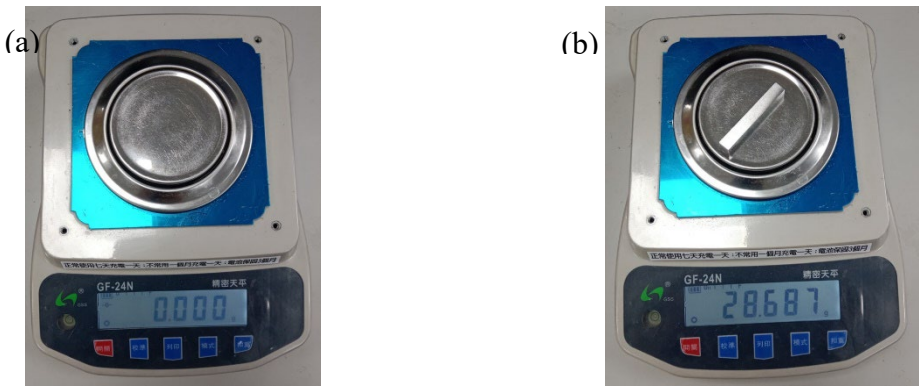

 doi:10.20944/preprints202402.0610.v1

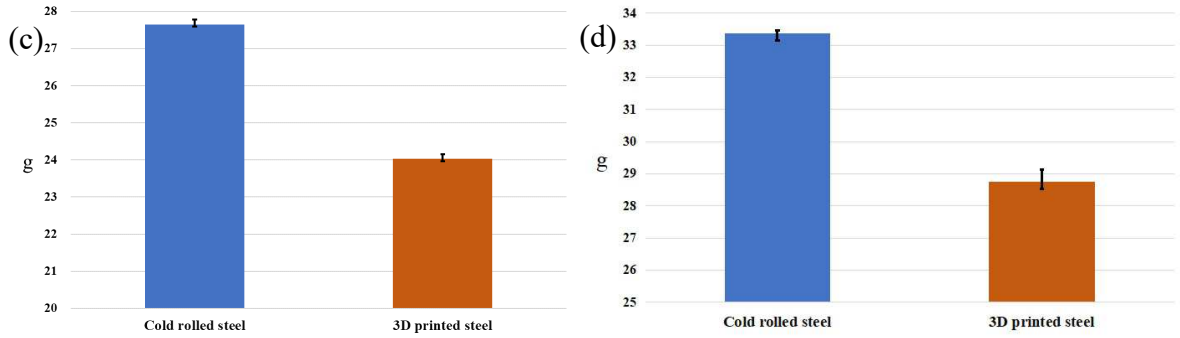

Figure 7. Digital precision weights and measuring instruments measure the weight. (a) represents no-loading in the weights and measures instrument. (b) represents the weight with the loading block specimen in the weights and measures instrument. (c) represents the weight of the tensile specimens. (d) represents the weight of the block specimens.

3.3. The Surface Roughness and Hardness Analyze

The performance of the metal surface roughness will affect the morphology and as-sembly capabilities of the parts. The surface hardness of metal materials will affect the plastic deformation ability in the part. The surface roughness of the 3D additive manufac-tured specimen is over 13μm in Ra and 88μm in Rz. The surface roughness is rougher than the general rolled steel from the morphology observed in Figure 4. Ding H. et al. [31] and Natali S. et al. [32] represent hybrid manufacturing to improve the efficiency and sur-face quality of the 3D additive manufactured specimens. Therefore, we used the milling process to process the surface in the additive manufactured specimen and the general rolled steel. Table 3 illustrates the conditions of milling processing. The purpose is to compare the performance in the surface roughness. The surface roughness index was measured by white light interferometry (ZYGO NewView8000). The material of the specimen is 316L SS. Figure 8a,b show the surface roughness in Ra and Rz when the block specimens were manufactured by 3D printing and rolled process and then pro-cessing in the surface of the block specimens by milling machine finishing. The surface roughness of 3D printing steel is 0.592μm and 2.941μm in Ra and Rz. The surface roughness of rolled manufactured steel is 1.269μm and 4.289μm in Ra and Rz. The ex-perimental results show that the workpiece of 3D printing can achieve the fineness of the general metal of 316L SS after secondary processing.

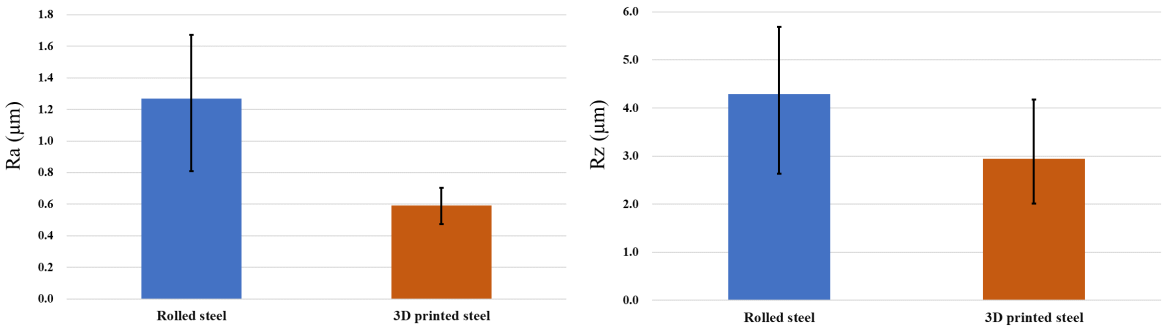

(a). The surface roughness in Ra (b). The surface roughness in Rz

Figure 8. The surface roughness in Ra and Rz after the milling machine cutting in the surface of the block specimens.

Table 3. The specimens process conditions by milling and grinding processing in the 316L SS.

Milling processing	Milling cutting tool Ø12 * Spindle speed 2,500rpm
Grinding processing	CBN 325N 100B Grinding wheel Ø180 * Rotating speed 2,500rpm

We use the grinding process to optimize the surface roughness in 3D additive speci-mens to verify that it can also be used in another machining process to improve the surface roughness

 doi:10.20944/preprints202402.0610.v1

performance. The diamond grinding wheel is CBN325N100B, and the grinding process method is shown in Table 3. Figure 9 shows the experimental results. We observed the surface roughness of the general rolled steel is 0.569μm and 3.104μm in Ra and Rz after grinding in the surface of the specimens. The surface roughness of the 3D printed steel is 0.202μm and 1.283μm in Ra and Rz after grinding in the surface of the specimens. The experimental results showed that the 3D-printed steel's surface roughness is higher. However, they can use different machining processes to optimize the surface roughness in the parts.

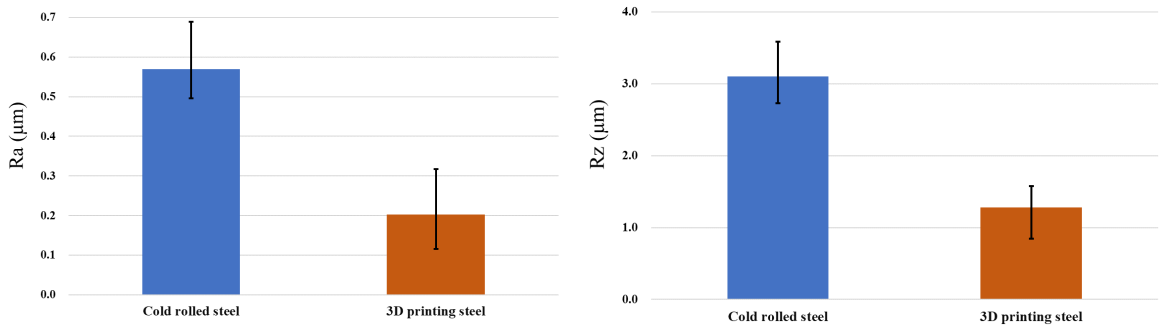

(a). The surface roughness in Ra. (b). The surface roughness in Rz.

Figure 9. The surface roughness in Ra and Rz after grinding in the surface of the block specimens.

The ratio of roughness depth Rz to the average surface roughness Ra represents the surface roughness performance. A high index in Rz/Ra is not suitable for application in aerospace and automobile parts [33]. Table 4 explains the performance of rolled and 3D printing steel in Rz/Ra. We observed that the surface roughness performance is better when 3D additive manufactured specimens are milled or ground on the surface. However, the Rz/Ra index was higher than that of general rolled steel. The 3D additive manufactur-ing process would produce pores in the specimens. Therefore, improving the pore in the part is a critical technology in 3D additive processing.

Table 4. Compare the performance of the surface roughness in Ra/Rz with 316L SS.

	Rz/Ra before milling or grinding	Rz/Ra after milling	Rz/Ra after grinding
3D additive steel	7.08~6.69	4.97	6.35
General rolled steel	-	3.38	5.46

In order to explore the reason why the performance of 3D printing steel is better than the general rolled steel in surface roughness after milling or grinding in the surface of the specimens, we used the FM-810e Microhardness tester to measure the hardness in the surface of the specimens as in Figure 10a. The measurement specimens were the general and 3D printing steel, as shown in Figure 4. Figure 10b is shown the measurement re-sults in the 3D printing steel. The hardness of HRC is about 35.3±3.0. Figure 10c is shown the measurement results in the general rolled steel. The hardness of HRC is about 28.3+3.0/-1.5. In addition, we also used a metal tensile tester to test the performance of 3D printing steel and the general rolled steel in the materials of 316L SS. The metal tensile tester was manufactured by Chun Yen Corp., as shown in Figure 10d. Figure 10e shows the experimental results of 3D printed and general rolled steel in the tensile strength and strain. We found that 3D printing steel is higher than general rolled steel in the hardness and tensile strength index. However, the elongation materials are only below 25% compared to the general rolled steel from the experimental results. This phenomenon is near the same as that of Basavraj, B. et al. [6]. It shows that the 3D printed steel belongs to hard and brittle materials, so they can use post-processing to optimize the surface roughness and fineness of the parts.

Preprints.org (www.preprints.org) | NOT PEER-REVIEWED | Posted: 12 February 2024 doi:10.20944/preprints202402.0610.v1

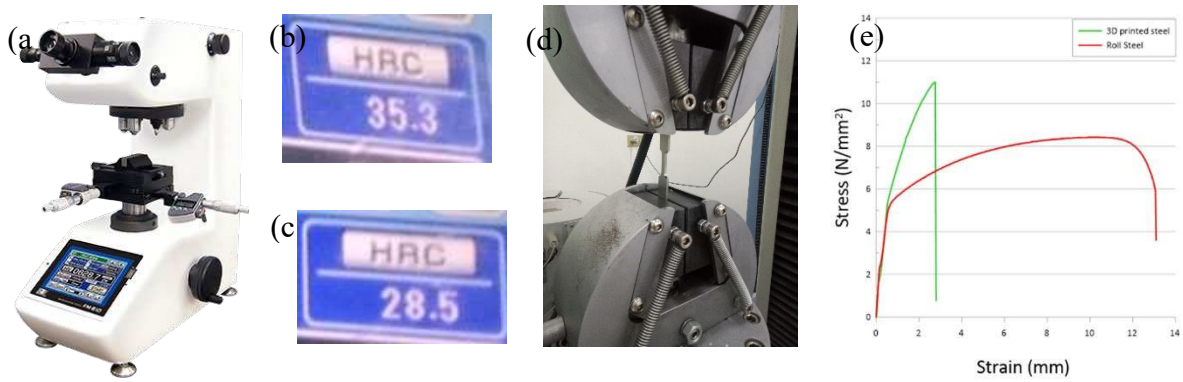

Figure 10. (a) is FM-810e Microhardness tester. (b) shows the hardness of 3D printed steel in the material of 316L SS. (c) shows the hardness of general rolled steel in the material of 316L SS. (d) is the tensile test. (e) is the relationship that stress and strain with the tensile specimens of 3D printed steel and rolled steel in the material of 316L SS.

3.4. The Performance of the Morphology

Figures 11 and 12 show the surface morphology when the specimens of 3D additive and general rolled steel were milled and ground on the surface. We observed that the index of 3D additive steel is higher than that of general rolled steel in Sz. It is due to the pore phenomenon during 3D additive printing [34]. The pore will increase the Sz index and reduce the specimen's weight. It may cause fatigue and cracks in the parts when the parts are used in the dynamic [35].

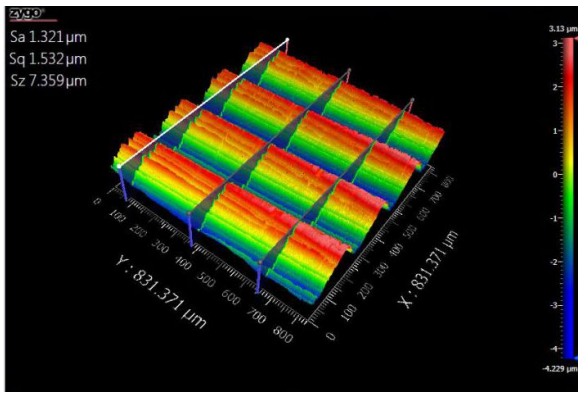

(a). The surface morphology of the block specimen when the block specimen is manufactured by 3D additive printing with 316L SS and the milling machine cutting in the surface of the block specimen.

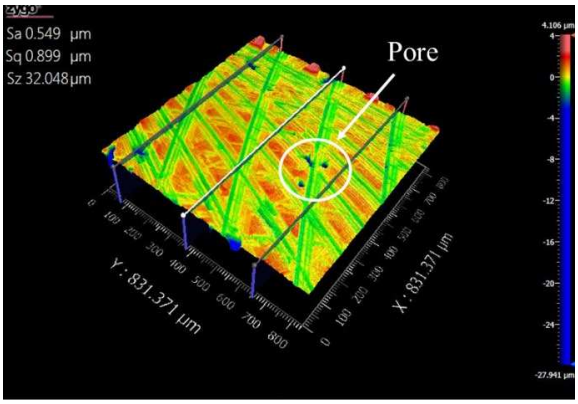

(b). The surface morphology of the block specimen when the block specimen is manufactured by roll process with 316L SS and the milling machine cutting in the surface of the block specimen.

Figure 11. The surface morphology of the block specimen when the block specimen manufactured by 3D additive printing and roll process after the milling machine cutting in the surface of the block specimen.

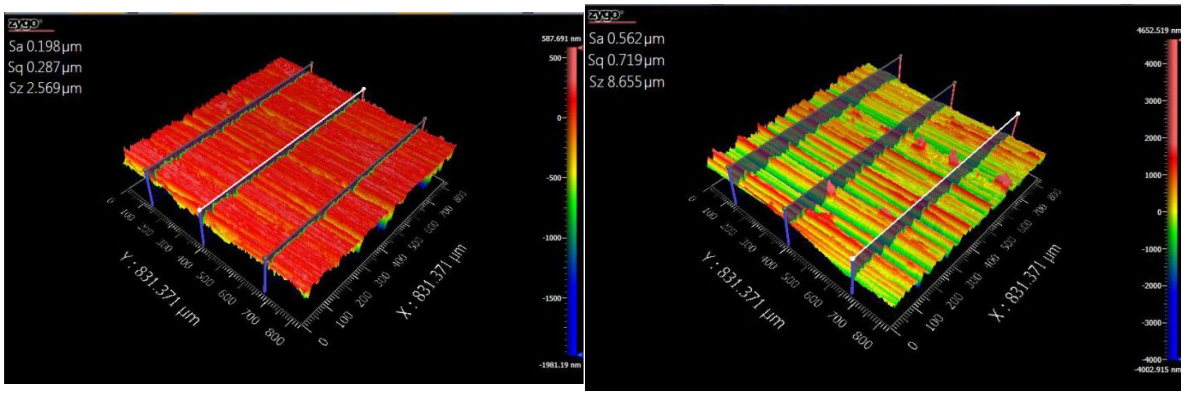

 doi:10.20944/preprints202402.0610.v1

(a). The surface morphology of the block specimen when the block specimen is manufactured by 3D additive printing with 316L SS and the grinding machine grinding in the surface of the block specimen.

(b). The surface morphology of the block specimen when the block specimen is manufactured by rolled process with 316L SS and the grinding machine grinding in the surface of the block specimen.

Figure 12. The surface morphology of the block specimen when the block specimen manufactured by 3D additive printing and rolled process after the grinding machine grinding in the surface of the block specimen.

4. Conclusions

Metal 3D printed technology has the advantages of faster prototypes, small batch production, no machining tools required, and significant material cutting loss. Therefore, they have been researched, developed, and applied extensively. However, this technology also has some porosity, surface roughness, and other performance issues. This study uses the milling and grinding process to improve the performance in the surface roughness of the workpiece. From the experimental results, we obtained some conclusions as below:

1) The workpiece will produce warpage and distortion in the metal 3D printed process. This is due to the uneven cooling phenomenon when the metal 3D printing process is under high-temperature sintering.
2) The workpiece of 3D printed is lighter 13.5±0.5% than the general rolled steel in the materials of 316L SS under the normal process manufactured.
3) The porosity of the workpiece will increase the index of Sz in surface roughness. This phenomenon will affect performance and surface morphology.
4) The performance of 3D-printed steel is better than that of general rolled steel in terms of tensile strength.
5) The hardness of 3D-printed workpieces is higher by 25% than that of general rolled steel, and the tensile strength is higher by 34%. However, the ductility and malleability of 3D-printed workpieces are only 21% compared to the general rolled steel in the 316L SS. Therefore, we found that a metal 3D-printed workpiece is a hard and brittle material compared to the general rolled steel [6].

We will study the following issues to explore the metal 3D printing process in the future:

1) Using different laser power and scanning speeds to improve the workpiece's porosity and strength.
2) Using heat treatment to explore the microstructure variation and the performance in the wear resistance.
3) Using the electroplating process to explore the ability and wear resistance of the electroplated layer to adhere to the surface of the 3D-printed workpiece.

Acknowledgments: The authors gratefully acknowledge the financial and information support provided to this study by National Science and Technology Council, Taiwan (NSTC 111-2222-E-231-002), National Chin-Yi University of Technology (NCUT 24-R-EP-010), Chien Hsin University of Science and Technology and WEN YANG Corp.

References

1. [1].Macdonald, E.; Wicker, R. Multiprocess 3D printing for increasing component functionality. Science, 2016, Vol. 353. Issue 6307: 1512.
2. [2].Iams, A. D.; Gao, M.Z.; Shetty, A.; Palmer, T.A. Influence of particle size on powder rheology and effects on mass flow during directed energy deposition additive manufacturing. Powder Technology, 2022, 396: 316-326.
3. [3].Wang, C.; Suder, W.; Ding, J.; Williams S. The effect of wire size on high deposition rate wire and plasma arc additive manufac-ture of Ti-6Al-4V. Journal of Materials Processing Technology, 2021, 288: 116842.
4. [4].John, J.; Mohsen, S. Metal additive manufacturing: a review of mechanical properties. Annual review of materials research, 2016, 46: 151-186.

5. [5].Terris, T.; Andreau, O.; Peyre, P.; Adamski, F.; Koutiri, I.; Gorny, C. Optimization and comparison of porosity rate measure-ment methods of Selective Laser Melted metallic parts. Additive Manufacturing, 2019, 28: 802-813.
6. [6].Basavraj, B.; Lekurwale, R. A review on advances in 3D metal printing. Materials Today: Proceedings, 2021, 45: 277-283.
7. [7].Chahal, V.; Taylor, R. M. Model Development for Residual Stress Consideration in Design for Laser Metal 3D Printing of Mar-aging Steel 300. In: 2018 International Solid Freeform Fabrication Symposium. University of Texas at Austin, 2018.
8. [8].Ngo, T.D.; Kashani, A.; Imbalzano, G.; Nguyen, K.T.Q.; Hui, D. Additive manufacturing (3D printing): A review of materials, methods, applications and challenges. Composites Part B: Engineering, 2018, 143: 172-196.
9. [9].Damian, P.; Radomir, M.; Lidia, M.P. Experimental research of surface roughness and surface texture after laser cladding. Ap-plied Surface Science, 2016, 388: 420-423.
10. [10].Zhang, S.; Hou, P.; Kang, J.; Li, T.; Mooraj, S.; Ren, Y.; Chen, C.H.; Hart, A.J.; Gerasimidis, S.; Chen, W. Laser additive manu-facturing for infrastructure repair: A case study of a deteriorated steel bridge beam. Journal of Materials Science & Technology, 2023, 154: 149-158.
11. [11].Zhong, Y.; Liu, L.; Wikman, S.; Cui, D.; Shen, Z. Intragranular cellular segregation network structure strengthening 316L stain-less steel prepared by selective laser melting. Journal of Nuclear Materials, 2016, 470: 170-178.
12. [12].Wang, Y.M.; Voisin, T.; McKeown, J.T.; Ye, J.; Calta, N.P.; Li, Z.; Zeng, Z.; Zhang, Y.; Chen, W.; Roehling, T.T.; Ott, R.T.; Santala, M.K.; Depond, P.J.; Matthews, M.J.; Hamza, A.V.; Zhu, T. Additively manufactured hierarchical stainless steels with high strength and ductility. Nature materials, 2017, 17.1: 63-71.
13. [13].Nath, S.D.; Irrinki, H.; Gupta, G.; Kearns, M.; Gulsoy, O.; Atre, S. Microstructure-property relationships of 420 stainless steel fabricated by laser-powder bed fusion. Powder Technology, 2019, 343: 738-746.
14. [14].Miranda, G.; Faria, S.; Bartolomeu, F.; Pinto, E.; Madeira, S.; Mateus, A.; Carreira, P.; Alves, N.; Silva, F.S.; Carvalho, O. Predic-tive models for physical and mechanical properties of 316L stainless steel produced by selective laser melting. Materials Science and Engineering: A, 2016, 657: 43-56.
15. [15].Pawan, T.; Tobias, G.; Christopher, R.; Francisco, G.M. Reducing surface roughness by chemical polishing of additively manu-factured 3D printed 316 stainless steel components. The International Journal of Advanced Manufacturing Technology, 2019, 100: 2895-2900.
16. [16].Penn, R. 3D printing of 316L stainless steel and its effect on microstructure and mechanical properties. 2017. PhD Thesis. Mon-tana Tech of the University of Montana.
17. [17].Hao, L.; Wang, W.; Zeng, J.; Song, M.; Chang, S.; Zhu, C. Effect of Scanning Speed and Laser Power on Formability, Micro-structure, and Quality of 316L Stainless Steel Prepared by Selective Laser Melting. Journal of Materials Research and Technology, 2023.
18. [18].Chahal, V.; Taylor, R.M. A review of geometric sensitivities in laser metal 3D printing. Virtual and Physical Prototyping, 2020, 15.2: 227-241.
19. [19].Bobbio, L.D.; Qin, S.; Dunbar, A.; Michaleris, P.; Beese, A.M. Characterization of the strength of support structures used in powder bed fusion additive manufacturing of Ti-6Al-4V. Additive Manufacturing, 2017, 14: 60-68.
20. [20].DIN EN ISO 25178-2:2020-02; Geometrische Produktspezifikation (GPS)—Oberflächenbeschaffenheit: Flächenhaft—Teil 2: Be-griffe, Definitionen Und Oberflächen-Kenngrößen (ISO/DIS 25178-2:2019). 2020.
21. [21].Bi, G.; Liu, S.; Su, S.; Wang, Z. Diamond grinding wheel condition monitoring based on acoustic emission signals. Sensors, 2021, 21.4: 1054.
22. [22].Dagmar, D.; Gabriela, I.; Janette, B.; Anna, G. The study of parameters of surface roughness by the correlation analysis. In: Materials Science Forum. Trans Tech Publications Ltd., 2015. p. 15-18.
23. [23].Lefky, C. S.; Zucker, B.; Wright, D.; Nassar, A.R.; Simpson, T.W.; Hildreth, O.J. Dissolvable supports in powder bed fu-sion-printed stainless steel. 3D Printing and Additive Manufacturing, 2017, 4.1: 3-11.
24. [24].Gan, M. X.; Wong, C.H. Practical support structures for selective laser melting. Journal of Materials Processing Technology, 2016, 238: 474-484.
25. [25].Zaeh, M. F.; Branner, G. Investigations on residual stresses and deformations in selective laser melting. Production Engineering, 2010, 4.1: 35-45.
26. [26].Liu, Y.; Yang, Y.; Wang, D. A study on the residual stress during selective laser melting (SLM) of metallic powder. The Interna-tional Journal of Advanced Manufacturing Technology, 2016, 87.1: 647-656.
27. [27].Maeda, A.; Jin, Y.; Kuboki, T. Light press of sheet metal edge for reducing residual stress generated by laser cutting considering mechanical properties and intensity of residual stress. Journal of Materials Processing Technology, 2015, 225: 178-184.

 doi:10.20944/preprints202402.0610.v1

28. [28].Almangour, B.; Grzesiak, D.; Yang, J.M. In-situ formation of novel TiC-particle-reinforced 316L stainless steel bulk-form com-posites by selective laser melting. Journal of Alloys and Compounds, 2017, 706: 409-418.
29. [29].Wu, Y.; Fang, J.; Wu, C.; Li, C.; Sun, G.; Li, Q. Additively manufactured materials and structures: A state-of-the-art review on their mechanical characteristics and energy absorption. International Journal of Mechanical Sciences, 2023, 108102.
30. [30].Fatemi, A.; Molaei, R.; Sharifimehr, S.; Phan, N.; Shamsaei, N. Multiaxial fatigue behavior of wrought and additive manufactured Ti-6Al-4V including surface finish effect. International Journal of Fatigue, 2017, 100: 347-366.
31. [31].Ding H.; Zou, B.; Wang, X.; Liu, J.; Li, L. Microstructure, mechanical properties and machinability of 316L stainless steel fabri-cated by direct energy deposition. International Journal of Mechanical Sciences, 2023, 243: 108046.
32. [32].Natali, S.; Brotzu, A.; Pilone, D. Comparison between mechanical properties and structures of a rolled and a 3D-printed stain-less steel. Materials, 2019, 12.23: 3867.
33. [33].Geier, N.; Pereszlai, C. Analysis of characteristics of surface roughness of machined CFRP composites. Periodica Polytechnica Mechanical Engineering, 2020, 64.1: 67-80.
34. [34].Zhang, C.; Jensen, D.J.; Yu, T. Effects of initial 3D printed microstructures on subsequent microstructural evolution in 316L stainless steel. Acta Materialia, 2023, 242: 118481.
35. [35].Yang, Y.; Gong, Y.; Qu, S.; Xie, H.; Cai, M.; Xu, Y. Densification, mechanical behaviors, and machining characteristics of 316L stainless steel in hybrid additive/subtractive manufacturing. The International Journal of Advanced Manufacturing Technology, 2020, 107: 177-189.366.